Forced autoionization

W. Sandner,* K. A. Safinya,† and T. F. Gallagher‡
Molecular Physics Laboratory, SRI International, Menlo Park, California 94025
(Received 21 August 1985)

We report an experimental and theoretical study of the forced autoionization of the doubly excited Ba $5d7d$ ($^1D_2$) state which lies ~ 200 cm^{-1} below the Ba$^+$ $6s_{1/2}$ ionization limit. In zero field the $5d7d$ state perturbs the $6snd$ ($^{1,3}D_2$) series by configuration interaction. The essential notion of forced autoionization is that applying a field of >2.5 kV/cm converts the $6snd$ states into a Stark continuum and the $5d7d$ state appears as an autoionization resonance. In this study we compare the zero-field configuration-interaction parameters with those obtained for the interaction of the $5d7d$ state with the structureless $|m|=1$ field-induced continuum and find rather similar values, thus confirming the utility of forced autoionization as a spectroscopic tool. In addition, we report a systematic investigation of the interaction of the $5d7d$ state with the highly structured $|m|=0$ Stark continuum.

I. INTRODUCTION

Configuration, or channel, interaction between a doubly excited state and a degenerate continuum is manifested in two ways. The first is the broadening of the doubly excited state by the autoionization to the degenerate continua. The second is that in a photoabsorption spectrum the doubly excited state appears as the Beutler-Fano profile characteristic of autoionizing states.[1] On the other hand, the interaction of the doubly excited state with a *series of bound Rydberg states* is manifested in both the perturbations of the energies of the Rydberg levels, corresponding to the autoionization width, and in a variation in the oscillator strengths corresponding to the Beutler-Fano profile of an autoionizing state.[1] Normally a doubly excited state can only exhibit one or the other of these pairs of phenomena. If, however, a strong electric field is used to artificially depress the ionization limit below the energy of a doubly excited state, the Rydberg series with which it interacts is converted to a continuum. In this case, the doubly excited state becomes an autoionizing state with a width reflecting the strength of the configuration interaction and a photoabsorption profile reflecting the zero-field oscillator strength distribution.

This phenomenon was first observed by Garton *et al.*,[2] who found in the absorption spectrum of shock-heated barium that the high-lying members of the principal series were not resolved for $n>12$, and that two known $5d8p$ doubly excited states appeared as asymmetric Beutler-Fano profiles. They suggested, correctly, that the fields produced in the shock heating turned $n>12$ states into a Stark continuum with the result that the $5d8p$ states appeared as autoionizing states. Accordingly, they termed the process "forced autoionization."

For more than a decade the subject was largely ignored, but the advent of the tunable laser and the ensuing interest in atomic Rydberg states led quite naturally to a renewed interest in forced autoionization. The recent experiments have verified in a thorough and controlled fashion that the original suggestion of Garton *et al.* was correct.[3–6] Furthermore, they have shown that, in addition to being an interesting phenomenon, it may in fact be a useful spectroscopic tool. Specifically, small perturbations which might otherwise go unnoticed in an optical spectrum are converted to easily detected forced autoionization profiles.[5]

With two exceptions,[3,6] all the previous work on forced autoionization has been carried out in such a way that the electric-field-induced continuum could be regarded as structureless. In fact, this is not always the case, as might be expected from the experimental studies of the Stark effect in alkali atoms in which long-lived Stark resonances have been observed above the depressed ionization limit in the electric field.[7,8]

Two works have been focused on the effects of the Stark resonances. We have already made a preliminary report of the positions of and intensity variations due to the Stark resonances in the observed spectra,[3] and subsequently Blondel *et al.*[6] showed that the locations corresponded to the results of previous alkali experiments. It is our purpose here to present a more detailed and expanded description of our investigations, thereby revealing most of the multilayered aspects of forced autoionization, which have not been fully appreciated in the past.

Specifically, we report the study of the forced autoionization of the Ba $5d7d$ ($^1D_2$) state which has a term energy of 41 841.6 cm^{-1}, 193.3 cm^{-1} below the zero-field ionization limit at 42 034.9 cm^{-1}.[9] In virtually any atom but hydrogen a state of binding energy W may be ionized by its classical ionization field F_c given by

$$F_c=(W/2)^2 , \tag{1}$$

where both F_c and W are given in atomic units. Equivalently, we may say that in a field F the classical field ionization limit I_c lies below the zero-field limit I_0 by $2F^{1/2}$, or

$$I_0-I_c=2F^{1/2} . \tag{2}$$

Again I_0 and I_c are given in atomic units. Using Eq.

(2), we can see that for $F > 2.3$ kV/cm, a modest field, the classical ionization limit lies below the $5d7d$ ($^1D_2$) state. Finally, the doubly excited $5d7d$ ($^1D_2$) state has the additional attraction of having been well studied by a number of experimental and theoretical techniques.[10–16]

It is useful to consider for a moment a qualitative picture of the Ba atom in a field of ~ 3 kV/cm. In Fig. 1 we sketch a cross section of the atom and the associated density of Stark states. Below the classical limit I_c the Stark states are spatially confined and thus bound. Above the classical limit there is a Stark continuum which may, under certain conditions, contain resonances corresponding to electron orbits localized on the cathode side of the atom. This is qualitatively indicated in the density of states on the right-hand side of Fig. 1. Although the field has an enormous impact on the Rydberg states converging to the Ba^+ $6s$ limit, it has little effect on the $5d7d$ state. The $5d7d$ state is in a potential analogous to the one shown in Fig. 1 but converging to one of the Ba^+ $5d$ limits 5000 cm^{-1} above the Ba^+ $6s$ limit. Thus the $5d7d$ state is bound by approximately 5000 cm^{-1}, and is thus constrained to have an orbital radius <40 a.u. which is hardly visible in Fig. 1. It is easy to show that such a tightly bound, spatially confined state is not directly affected by a field of 3 kV/cm.

With this picture it is now obvious how we were able to study experimentally the interaction of the isolated resonance with (a) a discrete Rydberg series of bound states under zero-field conditions, (b) a continuum with a uniform (energy independent) density of states at high-electric-field strength), and (c) a continuum with a nonuniform density of states at intermediate-field strengths.

Cases (a) and (b) (interaction with a discrete series and a flat continuum, respectively) are regularly encountered in atomic physics; here we investigate *the same* isolated resonance in both environments. Thereby, most importantly, we will find that the basic interaction parameters remain essentially unchanged. Such a result is hardly surprising today, because it was formulated as a cornerstone theorem in the development of multichannel quantum defect theory (MQDT).[17–19] In particular, it was used to draw a clear line of distinction between the channel interactions occurring at small radial distances, and the large-r boundary conditions which determine the discrete or continuous nature of a channel. In view of the extraordinary success of such a theorem, it is interesting to note that it was never directly demonstrated in a high-resolution experiment, simply because there is no direct experimental way of manipulating boundary conditions of a channel while leaving everything else (including an isolated perturber) truly unchanged. Forced autoionization may, under certain conditions, come closest to the experimental realization of this theoretical procedure, which will be discussed in Sec. III B.

Case (c) is different in a sense that, under zero-field conditions, creation of a *nonuniform density of continuum states* requires the interaction of at least two channels with different core configurations of the ion. Interaction of an isolated resonance with two such channels in Ba has recently been investigated by Gounand *et al.*[20] using MQDT techniques. In electric-field-induced continua

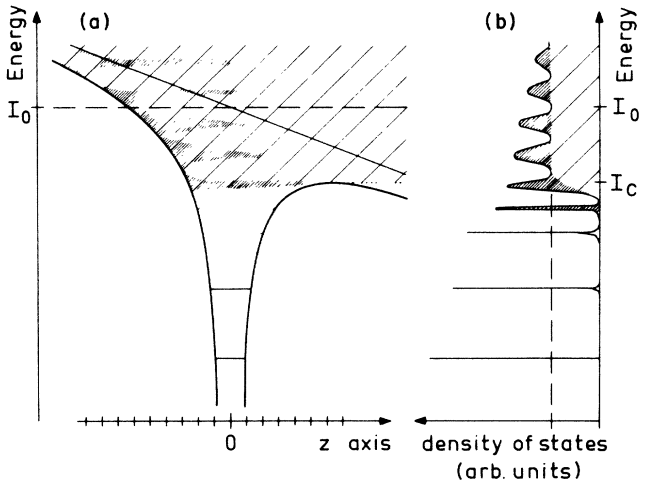

FIG. 1. (a) Schematic cross section through the potential surface of an atom in an external dc field. Shaded area: local density of quasistable states (Stark resonances) above and closely below the classical field ionization limit I_c. Hatched area: quasiuniform density of rapidly ionizing states. (b) Qualitative energy spectrum of the density of states emerging from (a), which is reflected in the photoabsorption cross section.

structures can occur and are, in fact, most common even if only one single core configuration is involved. A detailed experimental and theoretical study of forced autoionization into structured continua is given in Sec. III C.

Besides studying the interaction of the isolated resonance in different environments, we were also able to investigate its appearance under different excitation modes. These will affect the shape of the resonance, as commonly expressed by the Fano q parameter, and may lead to drastically different shapes of the observed signal, as will be shown in Sec. III A.

II. EXPERIMENTAL APPROACH

The apparatus which has been described before[21] consists of a crossed-beam arrangement. A collimated thermal beam of Ba, effusing from a heated stainless-steel tube, is intersected perpendicularly by two collinear pulsed laser beams. The interaction region is centered between parallel electric field plates, 1.08 cm apart, which provide either the controlled static electric field or, alternatively, a high-voltage field pulse. The latter is required for spectra taken under zero-field conditions and is typically delayed by several hundred nanoseconds with respect to the laser pulses. Created ions are accelerated through a grid in the upper-field plate and detected by a secondary-electron multiplier, whose output is fed into a gated integrator.

The pulsed dye lasers had typical bandwidths of $\Gamma_L \lesssim 1$ cm^{-1}; their frequency was monitored using a 3.54-cm^{-1} free-spectral-range étalon. The absolute frequency calibration has been obtained by connecting the relative frequency scale provided by the étalon with the well-known zero-field $J=2$ spectrum in Ba.[9] The spectra presented in this paper have been digitized by a computer and brought onto an absolute and linear energy scale, as indicated on the figures. Similarly, the absolute intensity of different spectra has been monitored during each run and normalized whenever necessary.

III. RESULTS AND DISCUSSION

A. Forced autoionization observed under different excitation schemes

Figure 2 shows the two excitation schemes involved in this experiment, whereas Fig. 3 displays typical zero-field and forced autoionization spectra obtained by using these excitations. Let us first consider excitation scheme A using the $6s6p$ ($^1P_1$) intermediate states. The zero-field spectrum obtained there is given in Fig. 3(a), exhibiting a series of bound states converging to the first ionization potential $I_0=42034.9$ cm^{-1} in Ba. We note a conspicuous "dip" in the absorption signal near the position of the $5d7d$ ($^1D_2$) perturber, which becomes in fact the dominant feature in the spectrum if we turn the bound Rydberg series into a continuum by application of an electric field [Fig. 3(b)]. The field of 4.8 kV/cm is high enough to field ionize essentially all states in this energy region, leaving only a relatively small modulation of the continuum absorption due to "Stark resonances," i.e., long-lived Stark states in the field. The modulation in the vicinity of the zero-field ionization limit was the focal point of a recent investigation from our laboratory.[22] In this section we will disregard any wiggly structure in the spectrum arising from Stark resonances and, instead, focus on the prominent asymmetric "window-type" resonance near 41 841 cm^{-1}, which represents the influence of the $5d7d$ ($^1D_2$) perturber on the field-induced continuum. Line shapes like the one seen in Fig. 3(b) are routinely encountered whenever an isolated bound state interacts with a neighboring continuum, and they are most conveniently characterized by means of a shape parameter q, introduced by Fano.[1] We will discuss the line shape in some detail below; here we simply note that a "window-type" resonance is characterized by $|q|<1$.

On first sight, a totally different situation is encountered when using the excitation path B. In the zero-field case [Fig. 3(c)] the bound Rydberg series is now concentrated in the very same region where there was the "dip" in the intensity distribution of Fig. 3(a). We also note strong peaks in the continuum, which show the presence of other bound-state perturbers. Turning on an electric field (7.5 kV/cm in this case) removes any difference in

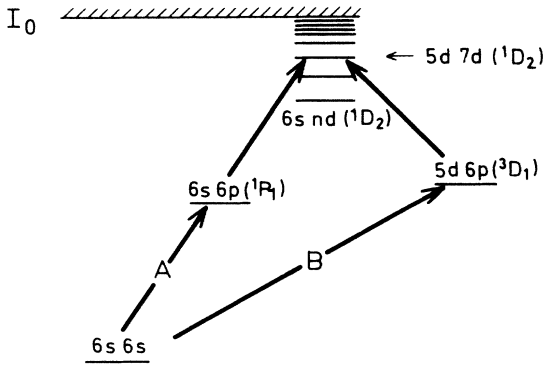

FIG. 2. Explanation of the two different excitation schemes A and B used in the present work.

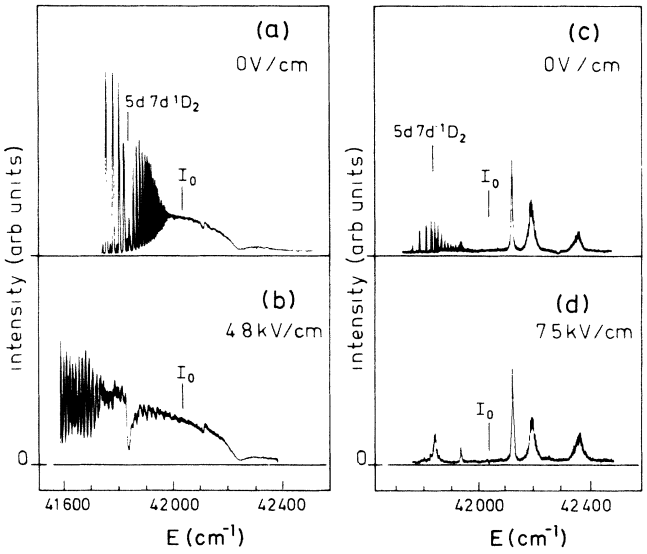

FIG. 3. (a) Photoabsorption spectrum observed in zero field, using excitation path A. (b) Same as (a), but observed at an applied dc electric field of 4.8 kV/cm. (c) Zero-field spectrum observed in path B. (d) Same as (c), but with an applied field of 7.5 kV/cm.

appearance between these "true" continuum resonances and the $5d7d$ ($^1D_2$) perturber, which now appears as a forced autoionization resonance characterized by a shape parameter $|q|\gg 1$, which denotes an almost Lorentzian-like line shape.

The difference in appearance of the forced autoionization resonance, when excited through either path A or path B, is easily understood from inspection of the respective intermediate states. As shown in Fig. 2, path A used the $6s$-$6p$ ($^1P_1$) transition as a first step, whereas path B first excites the $5d6p$ ($^3D_1$) intermediate state, which is dipole accessible through the $5d^2$ admixture in the Ba ground state.[23] These states serve as initial states for the second excitation step to the forced autoionization structure. Disregarding for the moment any structures in the field-induced continuum, $|\chi_E\rangle$, we may characterize the expected gross shape of the forced autoionization structure by its Fano-shape parameters $q^{(A)}$ and $q^{(B)}$, respectively, which are defined as[1]

$$q^{(A,B)}=\frac{\langle 5d7d\,|\,r\,|\,\Psi_i^{(A,B)}\rangle}{\pi V_E\langle\chi_E\,|\,r\,|\,\Psi_i^{(A,B)}\rangle}\ , \tag{3}$$

where $2\pi|V_E|^2=\Gamma_0$ is the width of the resonance. Inserting the exact[23] (configuration mixed) intermediate-state wave function $\Psi_i^{(A)}$,

$$\begin{aligned}|\Psi_i\rangle^{(A)}&=|\,6s\,6p(^1P_1)\rangle\\&=0.82\,|\,6snp\rangle+0.57\,|\,5dn'p\rangle+0.07\,|\,6pn''s,d\rangle\ ,\end{aligned} \tag{4}$$

we obtain an expression for $q^{(A)}$,

$$q^{(A)}=\frac{0.57}{0.82}\,\frac{\langle 5d7d\,|\,r\,|\,5dnp\rangle}{\pi V_E\langle\chi_E\,|\,r\,|\,6sn'p\rangle}\ , \tag{5}$$

where we have obeyed the dipole selection rules and kept

in mind that the continuum $|\chi_E\rangle$ belongs to a Ba^+ $(6s)$ ionic state. The square of the second factor, divided by $\pi/2$, is the ratio of dipole-allowed transition probabilities between two bound states (in the numerator) and between a bound state and a bandwidth Γ_0 of continuum states (in the denominator).[1] We may estimate this ratio to be in the order of unity, leaving us with an estimate for $q^{(A)}$,

$$|q^{(A)}| \lesssim 1 , \tag{6}$$

in good agreement with the experimental result of Fig. 3(b). In path *B*, on the other hand, the intermediate state $\Psi_i^{(B)}$ is an almost pure $5d6p$ configuration,[23]

$$|\Psi_i\rangle^{(B)} = |5d6p(^3D_1)\rangle = 0.99\,|5dnp\rangle + 0.09\,|5dn'f\rangle + 0.01\,|6pn''d\rangle . \tag{7}$$

Since this state is essentially not dipole connected to the Ba^+ $(6s)$ continuum, the denominator of (2) will become very small, leading to

$$|q^{(B)}| \gg 1 , \tag{8}$$

again in agreement with the experimental result [Fig. 3(d)]. Such a large q value describes an almost Lorentzian-like profile with maximum intensity near the center. Hence, this excitation scheme is best suited to study the interaction between any structures in the continuum and the isolated resonance, which will lead to conspicuous intensity fluctuations near the center of the resonance (cf. Sec. III C).

B. Forced autoionization into a smooth continuum: Comparison with zero-field data

In most practical cases of forced autoionization the electric field, which turns the bound Rydberg channel into a continuum will be low enough to leave the isolated resonance unaffected. In other words, the spatial region of the atom, where the resonant state is located, is dominated by internal atomic forces only, with the external field having a totally negligible effect. Hence, one would also expect the interaction between the isolated resonance and the neighboring channel to be totally unaffected by the electric field. Analysis of the spectra taken under zero-field conditions and in the presence of an electric field should consequently yield the same basic interaction parameters. Fano[24] and Harmin[25] have already shown in great detail how photoabsorption in the alkali atoms in the presence of an electric field can be broken up into two parts reflecting the two regions of space where the electric field is negligible (inner region) or dominant (outer region), respectively. Such an approach is the earmark of any quantum defect method which, on the other hand, is also the standard theory for analysis of the interaction of one isolated perturber with one or more neighboring channels. While, thus, a unified treatment of forced autoionization is possible, we prefer to break up the whole problem into smaller parts which will then be treated by much less sophisticated methods. In this section we consider the case of a spectrally flat field-induced continuum.

We start the discussion by observation of the fact that, experimentally, the bound $6snd$ Rydberg series of Ba can be turned into a *structureless continuum* by a suitable choice of electric field strength and light polarization. In particular, excitation in the presence of a 7.5-kV/cm electric field, using crossed linear polarization of both lasers, yielded a smooth continuum absorption signal from this channel in the energy region of the isolated resonance, which is about 200 cm^{-1} below the zero-field ionization limit. Physically this means that, under these conditions, the field ionization rate of all Stark levels of the atom is high enough to smear out any structure in the absorption spectrum. A field of 7.5 kV/cm, on the other hand, is still low enough for zero-field conditions to prevail for the interaction: The potential energy imposed by the field inside the radius $\langle r\rangle$ of the $7d$ state in $5d$ excited Ba [where $\langle r\rangle$ is known from Hartree-Fock (HF) calculations to be ~ 25 a.u.],

$$|E_{\text{field}}| \lesssim F\langle r\rangle \approx 3.6\times 10^{-5} \text{ a.u.} , \tag{9}$$

is in fact negligible when compared with the HF potential energy in the same region,

$$E_{\text{HF}} = -4\times 10^{-2} \text{ a.u.} . \tag{10}$$

The experimental result for the $5d7d$ $(^1D_2)$ forced autoionization peak, taken under these conditions and using excitation scheme *B*, is shown in Fig. 4(a). We find a smooth absorption profile with a slight asymmetry, which can be described by a Fano q parameter with high $|q|$, as was to be expected from considerations given earlier. The observed line shape contains negligible instrumental broadening due to the comparably high spectral resolution (~ 1 cm^{-1}) of the laser. Using Fano's familiar parametrization for this isolated resonance, we obtain the interaction parameters given in Table I. These parameters were obtained from a fitting procedure and fully describe the interaction of one isolated resonance with one continuum. In general, we would expect that the field-induced continuum contains parts which do not interact with our $5d7d$ $(^1D_2)$ perturber, giving rise to some constant background photoabsorption signal. This can in fact be seen in excitation path *A* [Fig. 3(b)], where the minimum in the signal does not go to zero as one would expect for a simple two-channel problem. In path *B*, all the continuum contributions are so small that their reliable determination from the spectrum was not possible in the present experiment.

The parameters describing the same interaction under zero-field conditions may be extracted from a most recent MQDT analysis of the perturbed $6snd$ $(^{1,3}D)$ bound-state series.[16] The results are also given in Table I. We note a rather good agreement in both the energy position and the width of the structure, confirming our initial expectation that the basic interaction parameters are not changed by the presence of an electric field.

In view of the preceding discussion, it may be surprising that the actual photoabsorption spectra with or without field [Figs. 3(c) and 3(d)] seem to differ more fundamentally than just by the fact that the energy scale is discrete in the one case and continuous in the other. In particular, the overall structure near the $5d7d$ $(^1D_2)$ ener-

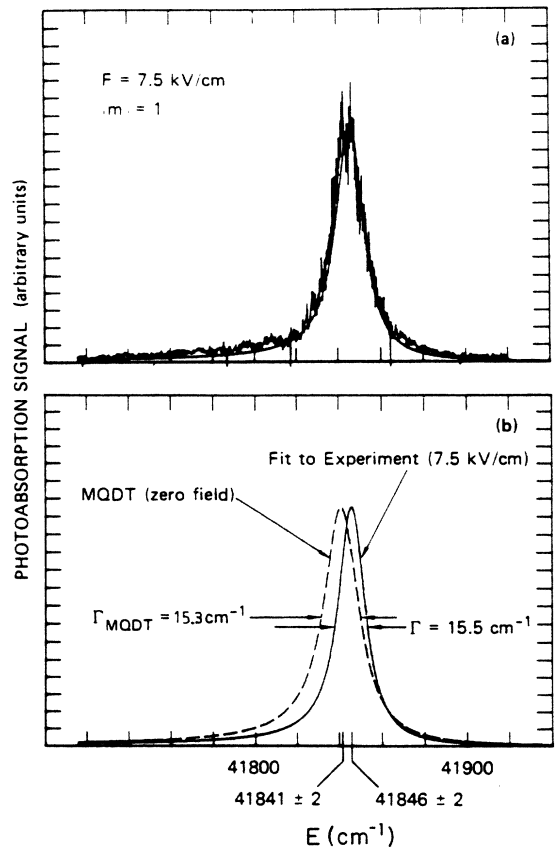

FIG. 4. (a) Expanded view of the forced autoionization structure of Fig. 3(d) around 41 841 cm^{-1}. Polarization of the two exciting lasers was crossed, yielding $|m|=1$ states only. (b) Solid line: fit to the experiment using $q^{(B)}=-25$ and $\Gamma_0=15.5$ cm^{-1}. Dashed line: Fano profile constructed from zero-field MQDT interaction parameters (cf. Table I), and using the same $q^{(B)}=-25$.

gy is wider and higher in the zero-field case, and, more seriously, it appears to be more asymmetric and even shifted with respect to the forced autoionization structure. All these observations, however, will be shown in the following to be in full agreement with theory, provided that all experimental factors are properly taken into account.

We consider the experimentally absorbed laser intensity under the various conditions of our experiment. In the discrete region (zero-field condition), the absorbed laser intensity I^{discr} is proportional to σ_n, the laser absorption cross section for the Rydberg state n, integrated over its line profile. Here and in the following we assume that the laser bandwidth Γ_L is large compared with the natural and Doppler linewidth of the state n. If we keep the laser at the energy E_n of the discrete state but replace the state itself by a continuum which does not vary much over the laser bandwidth, then the absorbed intensity I^{cont} will be proportional to $\Gamma_L\sigma(E_n)$, where $\sigma(E_n)$ is the absorption cross section in the continuum at the energy E_n. Hence, the ratio between the forced autoionization and a discrete line absorption, whenever the laser is tuned to the center energy E_n of a discrete line, is given by

$$\left.\frac{I^{\text{cont}}}{I^{\text{discr}}}\right|_{E=E_n}=\Gamma_L\frac{\sigma(E_n)}{\sigma_n}\ . \tag{11}$$

In a two-channel MQDT problem like the one considered here, the cross sections $\sigma(E_n)$ and σ_n obey the relation[19]

$$\sigma_n=\sigma(E_n)\left[\nu_0^3+\frac{d\mu_0}{d\nu_1}\nu_1^3\right]^{-1}, \tag{12}$$

where ν_0 and ν_1 are the effective quantum numbers relative to the Ba^+ $6s$ and Ba^+ $5d_{3/2}$ limit, respectively, and $d\mu_0/d\nu_1$ is the slope of a Lu-Fano plot which may conveniently be taken from Refs. 9 or 11. The expression in large parentheses represents the reciprocal width of a spectral band (in atomic units) associated with the discrete line n. From (12) we obtain for the absorption ratio

$$\left.\frac{I^{\text{cont}}}{I^{\text{discr}}}\right|_{E=E_n}=\Gamma_L\left[\nu_0^3+\frac{d\mu_0}{d\nu_1}\nu_1^3\right], \tag{13}$$

where the laser bandwidth Γ_L is understood to be given in atomic units.

In a final step we must consider a possible energy dependence in the detection of the laser absorption. In case of the forced autoionization we may assume an energy-independent detection efficiency: Each absorption process results in the instantaneous creation of a Ba^+ ion, either by direct photoionization (at energies far away from the center of the resonance), or by excitation and immediate autoionization ($\tau<10^{-12}$ sec) in the center of the resonance. In any case, the ions are accelerated by the prevailing dc field and detected by a multiplier. In the discrete spectrum, on the other hand, absorption takes place in zero field at time $t=t_0$, whereas the detection occurs at the time $t_{\text{det}}=t_0+\Delta t$, when a field pulse is applied to create the ions (after which the same considerations as above are valid). During the time interval Δt, however, a certain fraction of the excited atoms decays optically to lower-lying states, from which they can no longer be detected by field ionization. The optical decay rates vary strongly in the vicinity of the perturber, as has been demonstrated in a separate experiment.[11] Hence the detected signal S in the discrete spectrum differs from the absolute laser intensity I by an energy-dependent exponential decay factor

$$S^{\text{discr}}(E_n)=I^{\text{discr}}(E_n)e^{-\Delta t k_n}\ , \tag{14}$$

where the decay rates k_n of the states n are known experimentally.[11] In the forced autoionization case, on the other hand, we set the signal S equal to the absorbed intensity I.

TABLE I. Comparison of interaction parameters obtained from the photoabsorption in the presence of a dc electric field (forced autoionization), and in zero field, respectively.

	Forced autoionization	Zero-field MQDT
Resonance energy E_0 (cm^{-1})	41 846.3±2	41841±2[a]
Resonance width Γ_0 (cm^{-1})	15.5±1	15.3[b]
Asymmetry parameter $q^{(B)}$	−25	

[a]From Ref. 15.
[b]From Ref. 16.

Hence we obtain the final expression for the signal ratio at the energies of the discrete states E_n,

$$\left.\frac{S^{\text{cont}}}{S^{\text{discr}}}\right|_{E=E_n} = \Gamma_L \left[\nu_0^3 + \frac{d\mu_0}{d\nu_1}\nu_1^3\right] e^{\Delta t k_n} . \tag{15}$$

The right-hand side of Eq. (14) establishes the connection between the zero-field spectrum of Fig. 3(c) and the forced autoionization structure of Fig. 3(d). Since it is a nonlinear function of n, it accounts for the apparent distortions between the continuous Beutler-Fano profile and the envelope of the discrete spectrum recorded in the zero-field case. The validity of Eq. (15) may be demonstrated by reconstruction of a theoretical discrete spectrum $S^{\text{discr}}(E_n)$ from the observed forced autoionization profile $S^{\text{cont}}(E_n)$, sampled at the discrete energies E_n [we note, however, that only the line intensities of the interacting states could be computed; for states belonging to the noninteracting channel the corresponding continuous background signal $S^{\text{cont}}(E)$ has not been experimentally determined, as mentioned above]. The result is shown on Fig. 5, where typical values for $\Gamma_L = 1\ \text{cm}^{-1}$ and $\Delta t = 500$ nsec have been used. We find, by comparison with Figs. 3(c) and 3(d), that the intensity relation between the discrete spectrum and the forced autoionization is well described by Eq. (15).

The observations described in this section again lead to the conclusion that forced autoionization may be an useful experimental tool to determine interaction parameters in perturbed Rydberg series; in most cases it will be clearly easier to detect and analyze a Beutler-Fano autoionization profile in the continuum rather than small irregularities in the line positions of perturbed Rydberg series. We have demonstrated that, to a high precision, the forced autoionization structure and the perturbed Rydberg series bear the same information and may, in fact, be transformed into each other by application of standard MQDT methods. For this it is necessary that the experimental conditions are chosen such as to create a structureless field-induced continuum, and that the field is still low enough to leave the perturbing state unaffected. Both conditions are likely to be met in a large number of possible applications.

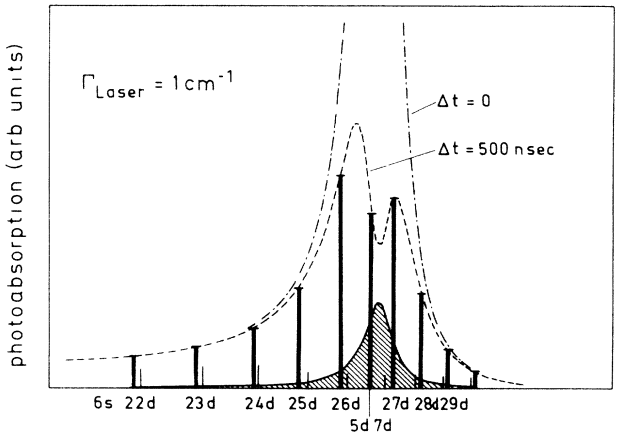

FIG. 5. Calculated discrete line intensities (bar spectrum), derived from the observed forced autoionization line shape (hatched area), and using Eq. (15). Envelope of the line intensities, using the parameters $\Gamma_L = 1\ \text{cm}^{-1}$, $\Delta t = 500$ nsec (dashed line), and $\Delta t = 0$ nsec (dash-dotted line) is also shown.

C. Forced autoionization into a structured field ionization continuum

In contrast to the preceding section, where the experimental conditions were chosen such as to suppress the occurrence of Stark resonances, we present in the following a detailed experimental study of the interplay between Stark resonances and the doubly excited autoionizing state.

Generally, we call Stark resonances any Stark states which are quasistable above the classical field ionization threshold given by Eq. (1). This threshold is a local saddle point in the combined Coulomb- and dc-field potential, above which an electron is classically free to escape to infinity. The lowest members of a Stark manifold belonging to a given principal quantum number n ionize completely at this threshold, while other Stark states persist at higher energies, forming resonances in the continuum of already ionized states. In any system except hydrogen the resonances are coupled to the degenerate continuum via the non-Coulombic part of the potential prevailing inside the atomic core.[26] This coupling gives rise to a finite lifetime of the resonances, resulting in a broad and even an asymmetric[27] line shape, phenomena which are also well known from zero-field autoionization.

Theoretically, the problem has been treated as channel interaction within the framework of quantum defect methods,[24,25] where the zero-field concept of a channel had to be modified according to the altered situation in the electric field. In particular, each Stark manifold of one given n value was treated as a separate channel. To each channel belongs a manifold of individual states, labeled by parabolic quantum numbers n,n_1,n_2, which interact with bound and continuum Stark states of neighboring n manifolds. The present problem contains, in addition, one doubly excited perturber within the infinite number of interacting n channels. This additional state changes the observed pattern of Stark levels in a rather dramatic way. We will show that the essential features of the complex experimental spectrum can be understood on the basis of a simple two-channel autoionization approach, where the only difference from zero-field autoionization is the phenomenological inclusion of Stark resonances as structures in the continuum channel.

1. Experimental results

A typical experimental spectrum of forced autoionization in the presence of Stark resonances is shown in Fig. 6(a). In contrast to Fig. 4(a), these data were taken at lower field strengths (4.8 kV/cm), and both lasers were polarized parallel to the electric field, resulting in a population of $|m| = 0$ states only. Under these conditions the presence of Stark resonances has been confirmed in previous experiments[22] and is obvious in the spectrum, most clearly on the low-energy side of the forced autoionization

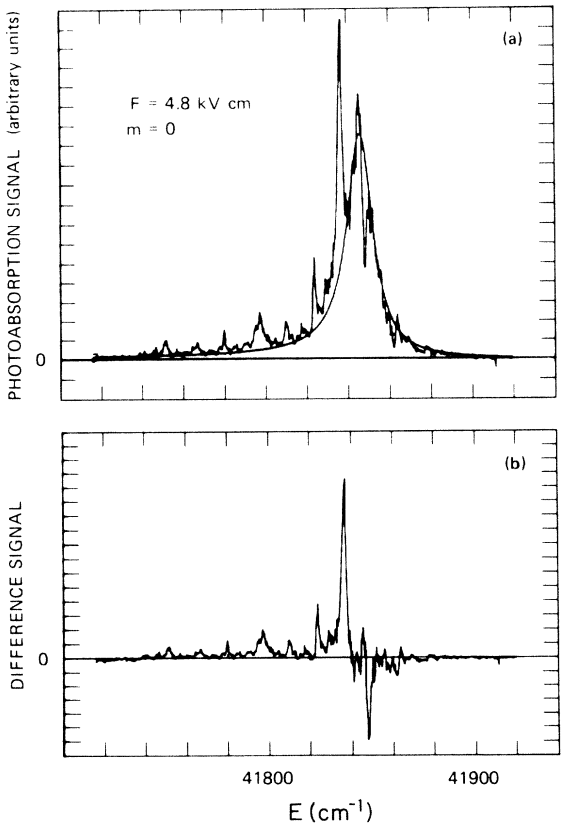

FIG. 6. (a) Same as in Fig. 4(a), but observed at field strength of 4.8 kV/cm, and with both laser polarizations parallel to the field ($m=0$ states only). Smooth line: fit curve from Fig. 4(b). (b) Difference between the experimental signal and the smooth Beutler-Fano profile in Fig. 4(b).

line. To focus on the effect of the Stark resonances only, we subtracted the analytical resonance-free line shape [fit curves in Fig. 4(b)] from the signal shown in Fig. 6(a). This approach serves best to demonstrate the effect of Stark resonances on the forced autoionization line. The difference signal may be viewed as consisting of a zero baseline, on which the Stark structures are superimposed as narrow structures in the absorption cross section [Fig. 6(b)]. It is apparent that the height of the Stark structures exhibits a dispersionlike behavior near the center of the resonance: Starting from low energies, their average height increases as they get closer to the center energy of the perturber at 41 846 cm^{-1}. In the immediate vicinity of this energy the amplitude in the difference spectrum changes sign, attains large negative values, and finally goes toward zero when the laser is scanned to higher energies, up to about 41 900 cm^{-1}.

This behavior of the Stark resonances in the difference spectrum of Fig. 6(b) is characteristic for an interference process. It is known[1] that, in a two-channel process, the excitation amplitude to the individual channels interfere with opposite phases on the two sides of a resonance. In the 7.5-kV/cm spectrum [Fig. 4(a)], this accounts for the slight asymmetry of the forced autoionization line shape, from which we deduce that in the present case the interference is destructive on the high-energy side of the perturber, and constructive on the low-energy side. Qualitatively, the same interference occurs at 4.8 kV/cm, as seen by dispersionlike amplitude of the Stark resonances. Moreover, the two-channel theory predicts the total signal to vanish identically at an energy $E_{\min}=E_0-\frac{1}{2}q\Gamma_0=42\,034$ cm^{-1}, which explains why the difference spectrum diminishes as the laser is scanned towards higher energies above 41 900 cm^{-1}.

To investigate the interference structure between the Stark resonances and the $5d7d$ perturber in greater detail, we took advantage of the fact that the Stark resonances can easily be moved in energy by comparatively small variations in the electric field strength. Starting from 4.8 kV/cm, we reduced the electric field strength in steps of 90 V/cm down to 3360 V/cm, taking a spectrum at each step. The resulting difference spectra [obtained again by subtracting the analytically known fit curve of Fig. 4(b) from the experimental signal] are shown on Figs. 7(a)—7(j). Presenting the data as differences between an

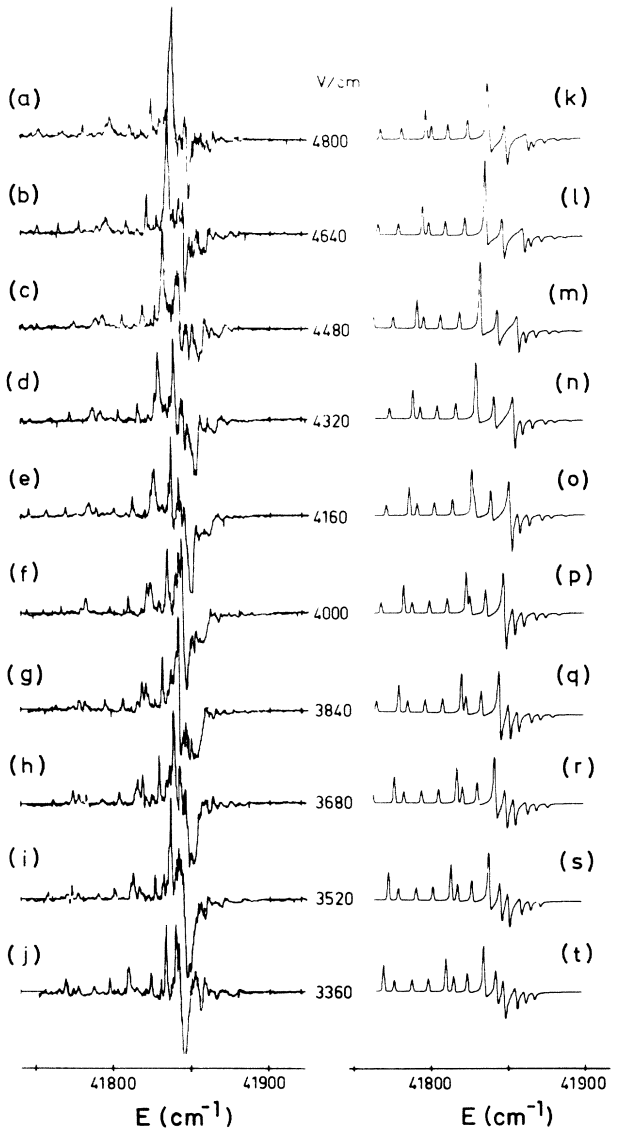

FIG. 7. (a)—(j): Same as Fig. 6(b), but observed under different field strengths. (k)—(t): Calculated spectra (for explanation see text).

experimental signal and an analytical nonlinear background structure of course requires both a careful calibration of the experimental energy scale and the intensities. However, a comparison of Fig. 6(a) with Fig. 6(b) reveals the advantage that the details of the interference phenomena are by far more obvious when presented as a difference spectrum.

From the spectra shown in Figs. 7(a)—7(j), both the energy positions and the amplitude of Stark resonances may be obtained as a function of the applied field strength. We use the field dependence of the energy positions to identify, at least approximately, some of the individual Stark resonances. The positions of the observed structures are plotted into an E-versus-F diagram of Fig. 8. In addition, the Stark levels (first order) of the hydrogenic manifolds belonging to $n=18$—23 are plotted into the same diagram. The comparison with hydrogenic Stark calculations would certainly be a gross oversimplification for field strengths *below* the classical field ionization limit: The large spatial extension of the Ba^+ core with its non-Coulombic forces will very effectively couple Stark manifolds of different n quantum numbers, which, in turn, result in pronounced avoided crossings. Hence the calculated lines in Fig. 8 are certainly not a good approximation in the region below the classical field ionization threshold. Above this threshold, however, where the present experiment has been carried out, the observed energy positions of the Stark structures exhibit a surprisingly simple pattern: at least for energies below 41 850 cm^{-1}, many of them follow the field dependence of the four or five "bluest" hydrogenic Stark states of a manifolds between $n=18$ and 20. Such a behavior is not totally unexpected: the very same coupling between the n manifolds that complicates the Stark spectra below the classical field ionization limit causes all but the few "bluest" states of each manifold to ionize above this limit. The remaining states possess rather similar slopes in the E-F diagram of Fig. 8, which allows them to move in energy without much mutual interaction. Effects of avoided crossings between states of different manifolds may still occur and can, for instance, be observed around 3.5 kV/cm between the states (18,17,0), (19,15,3), and (19,14,4), respectively. With increasing n, the spacing between adjacent n manifolds decreases, causing their quasistable bluest states to merge already at lower field strengths. Since they avoid crossing, they will approximately continue on parallel lines in an E-F diagram, with the common slope being that of a "medium" quasistable state with quantum numbers of, say, $(n, n_1=n-3, n_2=2)$. Around $n=21$ its slope is about 2.15×10^{-2} $cm^{-1}/$ (V/cm).

A careful experimental investigation of the Stark structures reveals individual slopes which agree very well with this qualitative picture (see Table II). Most of the structures could in fact be characterized by a linear field dependence, even though slight irregularities have been observed near the center energy of the perturber, where the interference pattern changes sign. In that case neither the maximum nor the minimum of the structure is known to be a good estimate for a resonance state position; rather it requires a complete analysis of the observed absorption profile to draw any conclusion on the resonance energy. The theoretical model presented in Sec. III C 2 assumes, as a starting point, a linear field dependence of the Stark state resonances in the absence of the perturber. It will be shown to reproduce the essential features of the observed interferences quite satisfactorily.

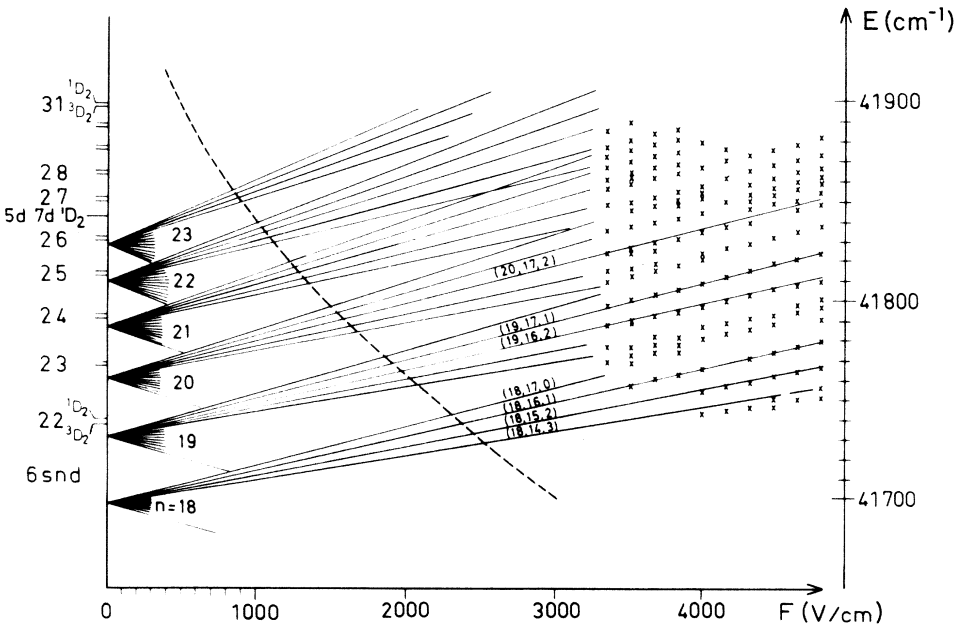

FIG. 8. E-vs-F diagram of the observed Stark resonances (crosses) in the present experiment. Dashed line: classical field ionization limit according to Eq. (1). Solid lines: Hydrogenic $m=0$ Stark manifolds (first order), labeled by parabolic quantum numbers (n,n_1,n_2). The energy positions of the Ba $6snd$ $^{1,3}D_2$ states are shown on the left ordinate for comparison.

TABLE II. Parameters used in the calculation of the interference pattern between Stark resonances and the main forced autoionization peak.

Stark resonance labels k	Energy position at 3360 V/cm (cm^{-1})	Slope dE/dF $\left[10^{-2}\frac{cm^{-1}}{V/cm}\right]$	Relative peak intensity B_k (arb. units)	Width G_k (cm^{-1})	Relative peak interaction strength A_k (arb. units)
1	41 735.9	1.11	10	1.0	0.1
2	41 745.5	1.47	10	1.0	0.1
3	41 755.1	1.75	10	1.0	0.1
4	41 768.8	1.90	17.5	1.0	0.175
5	41 775.7	1.67	10	1.0	0.1
6	41 787.3	1.61	10	1.0	0.1
7	41 797.8	1.78	10	1.0	0.1
8	41 809.2	1.94	17.5	1.0	0.175
9	41 814.2	1.52	10	1.0	0.1
10	41 823.1	1.74	10	1.0	0.1
11	31 833.8	1.99	17.5	1.0	0.175
12	41 842.0	1.66	10	1.0	0.1
13	41 847.2	1.79	10	1.0	0.1
14	41 855.2	1.83	10	1.0	0.1
15	41 860.9	1.86	10	1.0	0.1
16	41 866.6	2.29	10	1.0	0.1
17	41 871.8	2.60	10	1.0	0.1
18	41 877.5	2.16	10	1.0	0.1

2. *Theory*

In Sec. II B it has been shown that the forced autoionization profile observed there may well be described using a simple two-channel approach, at least as long as the continuum is spectrally flat (i.e., no Stark resonances are present). Moreover, it has already been pointed out that any m-channel theory, containing one perturber and $m-1$ electric-field-induced continua (labeled, for instance, by the principal quantum numbers n of field ionized Stark manifolds[24]), would always reduce to an effective two-channel problem in the present experiment. This is because in the excitation scheme B used here the direct continuum excitation amplitude is extremely small.

In order to account theoretically for the observed interference structures between the bound-state perturber $5d7d\ (^1D_2)$ and the field-induced Stark continuum, we introduce the following formal two-channel problem: Channel 1 is represented by the bound-state perturber $|\rho\rangle$, localized at energy E_ρ. Channel 2, the Stark continuum, is represented by a continuous wave function $|\chi_E\rangle$, whose spectral density exhibits structures which will be identified as Stark resonances. In an exact treatment, the function $|\chi_E\rangle$ has to be replaced by a multichannel wave function which contains the effects of the mutual interaction between the individual n manifolds in an electric field. The result of an exact diagonalization of that part of the Hamiltonian is expected to yield irregular and asymmetric line shapes of the Stark resonances, as seen in previous experiments. In the present case, the line shape of the Stark resonances is both affected by interaction with neighboring Stark manifolds *and* the interaction V_E with the bound-state perturber $|\rho\rangle$. In order to focus on the latter, we make the simplifying assumption that (a) the Stark resonances k in channel 2 have symmetric Lorentzian shapes, and (b) their individual widths Γ_k are equal and denoted by Γ in the following. The energy positions E_k are taken from the experiment (cf. Fig. 8).

The total wave function Ψ_E is obtained in the usual manner as a superposition of the two-channel wave functions,[1]

$$\Psi_E = a\rho + \int dE' b_{E'} \chi_{E'} \ . \tag{16}$$

The reduced absorption intensity (that is, the observed absorption from an initial state $|i\rangle$ to the exact states $|\Psi_E\rangle$, divided by the absorption to the pure continuum channel $|\chi_E\rangle$) can be expressed as follows:

$$\frac{|\langle\Psi_E|T|i\rangle|^2}{|\langle\chi_E|T|i\rangle|^2} = \frac{(q+\epsilon)^2}{1+\epsilon^2} \ , \tag{17a}$$

with

$$q = \frac{\langle\rho|T|i\rangle}{\pi V_E^* T_{iE}} + \frac{1}{\pi V_E^* T_{iE}} \mathrm{P}\int \frac{V_{E'}^* T_{iE'}}{E-E'} dE'$$

$$= q^0 + \frac{1}{\pi V_E^* T_{iE}} \rho(E) \ , \tag{17b}$$

and

$$\epsilon = \frac{E-E_\rho}{\pi|V_E|^2} - \frac{1}{\pi|V_E|^2} \mathrm{P}\int \frac{|V_E|^2}{E-E'} dE'$$

$$= \epsilon^0 - \frac{1}{\pi|V_E|^2} \mathcal{F}(E) \tag{17c}$$

(with the shorthand notation $T_{iE}=\langle\chi_E \mid T \mid i\rangle$).

In those cases where the energy dependence of V_E and T_{iE} can be neglected (which is true for practically all cases of zero-field atomic configuration interaction) the principal part integrals $\rho(E)$ and $\mathcal{F}(E)$ vanish identically. This leads to the parametrization of the familiar Beutler-Fano resonances in terms of an energy-independent shape parameter q^0 and a reduced energy scale ϵ^0, where the latter is connected with the experimental energy scale E through a linear transformation.[1] Inclusion of the principal part value integrals, on the other hand, introduces an energy dependence in q and causes ϵ to be nonlinear in E, thus allowing for the increased complexity of the spectrum in the case of a structured continuum $|\chi_E\rangle$.

Specifically, we make the following ansatz for the interaction matrix element V_E:

$$V_E=\langle\chi_E \mid H \mid \rho\rangle=V_E^0\left[1+\sum_k A_k\frac{(\frac{1}{2}\Gamma)^2}{(E-E_k)^2+(\frac{1}{2}\Gamma)^2}\right]. \tag{18}$$

The expression in large parentheses reflects our initial assumptions on the energy dependence of the electric-field-induced continuum wave function $|\chi_E\rangle$: it is composed of a constant part plus a sum over Lorentzians, located at energies E_k with an adjustable amplitude A_k and a common width Γ. V_E^0 here is the energy-independent configuration-interaction strength with the flat part of the Stark continuum. Similarly, the absorption matrix element reads

$$T_{iE}=\langle\chi_E \mid T \mid i\rangle=T_{iE}^0\left[1+\sum_k B_k\frac{(\frac{1}{2}\Gamma)^2}{(E-E_k)^2+(\frac{1}{2}\Gamma)^2}\right], \tag{19}$$

where B_k is again an adjustable parameter to account for variation in the apparent amplitude of individual Stark resonances. We require the amplitudes B_k of the energy-dependent part in T_{iE} to be strictly proportional to the amplitudes A_k in V_E:

$$A_k=\alpha B_k\ . \tag{20}$$

Equation (20) reflects the assumption that both energy dependences (18) and (19) have their common origin in the variation of the density of Stark states $|\chi_E\rangle$.

Inserting (18) and (19) into (17a), one finds an analytical expression for the principal part integrals in (17b) and (17c), which finally yields the expressions for the unknown energy-dependent quantities q and ϵ:

$$q(E)=\frac{1}{[1+\Lambda(E)][1+\alpha\Lambda(E)]}\times\left[q^0+2\sum_j\left[\frac{\alpha+1}{2}\beta_j(E)+\alpha\lambda_j(E)\right]\right], \tag{21a}$$

and

$$\epsilon(E)=\frac{1}{[1+\alpha\Lambda(E)]^2}\left[\epsilon^0+2\sum_j[\alpha\beta_j(E)+\alpha^2\lambda_j(E)]\right]. \tag{21b}$$

Here we have defined

$$\Lambda(E)=\sum_j\frac{B_j}{\eta_j^2+1}\ , \tag{22a}$$

$$\beta_j(E)=\frac{B_j\eta_j}{\eta_j^2+1}\ , \tag{22b}$$

$$\lambda_j(E)=B_j^2\left[\frac{1}{4}\eta_j\frac{\eta_j^2+3}{(\eta_j^2+2)^2}\right]+\sum_{j'\neq j}\frac{2B_jB_{j'}(\eta_j\eta_{jj'}+2)}{\eta_{jj'}[(\eta_j\eta_{jj'}+2)^2+(2\eta_j-\eta_{jj'})^2]}\ , \tag{22c}$$

with the reduced energies η_j and $\eta_{jj'}$ being

$$\eta_j=\frac{E-E_j}{\frac{1}{2}\Gamma} \tag{22d}$$

and

$$\eta_{jj'}=\frac{E_j-E_{j'}}{\frac{1}{2}\Gamma}\ ,$$

respectively. Insertion of (21a) and (21b) into (17a) yields the expression for the forced autoionization spectrum. The result of the calculation [after subtraction of the Beutler-Fano line shape of Fig. 4(b)] is shown on the right-hand side of Figs. 7(k)—7(t). The parameters used are given in Table II. Basically, the choice of parameters follows immediately from inspection of one of the spectra of Figs. 7(a)—7(j). Once the set of parameters has been fixed, the other spectra follow from the theoretical expressions given above.

As for comparison between theory and experiment, we note the following points.

(a) The dispersionlike behavior of the Stark resonances is clearly reproduced. That is, the Stark resonances add to the forced autoionization structure on its low-energy wing, whereas they appear inverted, as "holes" in the forced autoionization peak, on its high-energy wing. The transition from a positive peak to a negative hole structure occurs within a narrow energy range. A particularly conspicuous result is obtained if the field strength is chosen such that one Stark resonance is located right in the center of the forced autoionization peak, as it happens to be the case at $F=4000$ V/cm: We find from the calculations and, maybe even more dramatically in the experiment, that the transition from a high positive to an equally large negative structure changes within the width of one Stark resonances (1 cm^{-1}). Speaking in terms of q parameters for the Stark resonances, one would say that q changes from $|q|\gg 1$ on the low-energy wing of the forced autoionization peak to $|q|\ll 1$ on its high-energy wing, with $q=1$ near the center of the perturber.

(b) The disappearance of any structure near 41 900 cm^{-1} is also reproduced, which is clearly related to the

minimum in the underlying Beutler-Fano profile of the forced autoionization peak. Calculations (not shown in Fig. 7) prove that the Stark resonances recover as peaks at even higher energies, as one would expect.

(c) Details of the widths of the Stark structures are not reproduced by theory. In particular, various individual resonances seem to merge into one big hole structure on the high-energy side of the perturber, while they remain clearly distinguishable in the calculated spectra. These details are beyond the scope of the present calculations. As a consequence, there remains a certain freedom in the choice of the fit parameters A_k and B_k, since their influence on the overall quality of the fit is not independent of each other. This explains why we obtained $A_k = 1 \pm 0.3$ with constant B_k in our preliminary study[3] (which corresponds to $C = 2 \pm 0.3$ in the notation given there), while the refined examination described in the present work rather suggests a variable B_k and a generally smaller A_k to be chosen. We emphasize, however, that both parameters are rather phenomenological and only serve to account for the structures in the density of continuum states which, in turn, reflect the existence of Stark resonances. The main objective of the present work was to show that the phenomenological inclusion of a structured continuum within the framework of configuration-interaction theory already accounts for the essential features of the experiment. Hence, despite its simplicity, the theory still allows considerable insight into the rather complex absorption spectra which one obtains in the region where both autoionization and Stark resonances are present.

IV. CONCLUSION

In this experimental and theoretical study we have investigated several facets of forced autoionization, which has enabled us to reach a fairly complete understanding of the process. First, in view of the internal consistency and comprehensiveness of the present study, it was important that we were able to excite predominantly either the continuum or the discrete $5d7d$ state by the choice of the intermediate state. Second, the careful study of the interaction of the $5d7d$ state with the structureless $|m| = 1$ continuum allowed a detailed comparison with the analogous interaction in zero electric field, and we found similar configuration-interaction parameters. Third, the unique and central feature of this work is the study of the forced autoionization of the $5d7d$ state to the highly structured $|m| = 0$ Stark continuum in which we were able to scan the Stark resonances through the $5d7d$ state at will by small changes in the applied electric field. In spite of the complexity of the observed spectra we were able to fit all the observations quite satisfactorily to a simple, physically appealing model based on the hydrogenic Stark effect and configuration-interaction theory. In fact, this application of the configuration-interaction theory demonstrates its applicability to the interaction with a strongly energy-dependent continuum, which is a rather uncommon case in zero-field atomic physics. Finally, we are led to the conclusion that forced autoionization is a useful spectroscopic tool and is quite interesting in its own right.

ACKNOWLEDGMENTS

This work was supported by the Department of Energy, Office of Basic Energy Sciences, Division of Chemical Sciences. We are pleased to acknowledge stimulating and useful discussions with D. L. Huestis, A. F. Starace, and R. J. Champeau, and the assistance of L. Dube in clarifying some mathematical details. One of us (W.S.) thanks the Deutsche Forschungsgemeinschaft for financial support.

*Present address: Fakulät für Physik, Hermann-Herder-Strasse 3, D-7800 Freiburg, West Germany.

†Present address: Schlumberger-Doll Research, Old Quarry Road, Ridgefield, CT 06877.

‡Present address: Department of Physics, University of Virginia, Charlottesville, VA 22901.

[1]U. Fano, Phys. Rev. **124**, 1866 (1961).

[2]W. R. S. Garton, W. H. Parkinson, and E. M. Reeves, Proc. Phys. Soc. London **80**, 860 (1962).

[3]W. Sandner, K. A. Safinya, and T. F. Gallagher, Phys. Rev. A **24**, 1647 (1981).

[4]B. E. Cole, J. W. Cooper, and E. B. Saloman, Phys. Rev. Lett. **45**, 887 (1980).

[5]T. F. Gallagher, F. Gounand, R. Kachru, N. H. Tran, and P. Pillet, Phys. Rev. A **27**, 2485 (1983).

[6]C. Blondel, R. J. Champeau, and C. Delsart, Phys. Rev. A **27**, 583 (1983).

[7]R. R. Freeman and N. Economou, Phys. Rev. A **20**, 2356 (1979).

[8]P. Jacquinot, S. Liberman, and J. Pinard, in *Etats Atomiques et Moleculaires Couples a un Continuum. Atomes et Molecules Hautement Excites,* edited by S. Feneuille and J. C. Lehman (CNRS, Paris, 1978).

[9]M. Aymar, P. Camus, M. Dieulien, and C. Morillon, Phys. Rev. A **18**, 2173 (1978).

[10]J. R. Rubbmark, S. A. Borgstrom, and K. Bockasten, J. Phys. B **10**, 421 (1977).

[11]T. F. Gallagher, W. Sandner, and K. A. Safinya, Phys. Rev. A **23**, 2969 (1981).

[12]M. Aymar, P. Grafstrom, C. Levison, H. Lundberg, L. Nilsson, and S. Svanberg, Z. Phys. A **303**, 1 (1981).

[13]E. Matthias, P. Zoller, D. S. Elliot, N. D. Piltch, S. J. Smith, and G. Lendis, Phys. Rev. Lett. **50**, 1914 (1983).

[14]O. C. Mullins, Y. Zhu, and T. F. Gallagher, Phys. Rev. A **32**, 243 (1985).

[15]M. Aymar and O. Robeax, J. Phys. B **12**, 531 (1979).

[16]A. Guisti-Suzor and U. Fano, J. Phys. B **17**, 4277 (1984).

[17]M. J. Seaton, Proc. Phys. Soc. London **88**, 801 (1966).

[18]M. J. Seaton, Rep. Prog. Phys. **46**, 167 (1983).

[19]U. Fano, Phys. Rev. A **2**, 353 (1970).

[20]F. Gounand, T. F. Gallagher, W. Sandner, K. A. Safinya, and R. Kachru, Phys. Rev. A **27**, 1925 (1983).

[21]T. F. Gallagher, L. M. Humphrey, R. M. Hill, W. E. Cooke, and S. A. Edelstein, Phys. Rev. A **16**, 1098 (1977).

[22]W. Sandner, K. S. Safinya, and T. F. Gallagher, Phys. Rev. A **23**, 2448 (1981).

[23]H. Friedrich and E. Trefftz, J. Quant. Spectrosc. Radiat. Transfer **9**, 333 (1969).
[24]U. Fano, Phys. Rev. A **24**, 619 (1981).
[25]D. A. Harmin, Phys. Rev. A **26**, 2656 (1982).
[26]M. G. Littman, M. M. Kash, and D. Kleppner, Phys. Rev. Lett. **41**, 103 (1978).
[27]S. Feneuille, S. Liberman, J. Pinard, and A. Taleb, Phys. Rev. Lett. **42**, 1404 (1979).